ELSEVIER

Journal of Photochemistry and Photobiology A: Chemistry 115 (1998) 21–26

Journal of Photochemistry and Photobiology A:Chemistry

Sensitized luminescence of Eu^{3+}/Gd^{3+}/cinnamic acid mixed complex

János Erostyák *, Andrea Buzády, István Hornyák, László Kozma

Department of Experimental Physics, Janus Pannonius University, Ifjúság u. 6., Pécs H-7624, Hungary

Received 18 September 1997; received in revised form 23 January 1998; accepted 26 January 1998

Abstract

The photoluminescence of europium and gadolinium mixed complexes with cinnamic acid is investigated at room temperature. The maximum emission intensity is found to be at 70% Eu^{3+}/30% Gd^{3+} content. The probable ways of energy transfer processes are discussed on the basis of spectroscopic data. Photochemical degradation of the sample is found, the degree of which depends on the Eu^{3+}/Gd^{3+} ratio.

Keywords: Intramolecular energy transfer; Sensitized luminescence of Eu^{3+}; Time-resolved luminescence; Photochemical degradation

1. Introduction

The complexes of lanthanides have characteristic luminescence properties due to the intra-, and intermolecular energy transfer processes. Using their narrow-band, long-lifetime emission they are widely applied in fluoroimmonoassays, as luminescent probes or as luminescent display materials, etc. [1–7]. These complexes have a central lanthanide ion and one or more type of organic ligands. The basic steps of the energy transfer are the following. The excitation light is absorbed by the ligands, which can relax to the ground state by radiative and non-radiative transitions or to the triplet states by intersystem-crossing (ISC). The energy from the triplet state of the ligand can be transferred to the lanthanide ion by intramolecular energy transfer, which relaxes also by radiative and non-radiative transitions. The lanthanide emission has narrow spectral bandwidth, long lifetime and lies spectrally far from the emission of the ligand. From the point of view of applications, the most important task is to produce emission intensity as high as possible. To do this, the complexes can have, i.e., different kinds of ligands [8] or complexes of different lanthanides can be mixed [9]. In these cases, over the intra- and intermolecular energy transfer processes the competition of different quenching and shielding effects influences the yield of the whole energy transfer circle [10–13]. In this paper, the luminescence properties of the mixed complexes of Eu^{3+}/(cinnamic acid)$_3$ and Gd^{3+}/(cinnamic acid)$_3$—(Eu/Gd/CA) stands below for them—are reported.

2. Experimental details

The CA was at first neutralized by NaOH, then the water solution of $Eu(NO_3)_3 \cdot 6H_2O$ and $Gd(NO_3)_3 \cdot 6H_2O$ were added into CA solution in mole ratio of 1:3 of lanthanides and CA meanwhile mixing. A white precipitate was received. The product was filtered and washed by bidistilled water, then dried in vacuum at 80°C. A series of mixed complexes was prepared in which the Eu^{3+} content was gradually decreased and the Gd^{3+} content was increased. The formulas of mixed complexes are listed in Table 1. The materials were used in powder form for the measurements.

The luminescence measurements (emission and excitation spectra, decay curves) were carried out by a Perkin-Elmer LS50B luminescence spectrometer at room temperature using its solid sample holder. This spectrometer has a Xe flash lamp as excitation source. The time resolution of the instrument is 10 μs. The spectra were measured in phosphorescence mode, with an integrating gate of 5 ms. The luminescence of Eu^{3+} has a decay time of around 0.8 ms, thus the gate of 5 ms is long enough to integrate all the signals after the excitations. To determine the decay times the decay curves were measured in 10 μs steps, which gives an excellent resolution when measuring sub-microsecond decays. The I_0 initial intensities (see Section 3.3) were measured in fluorescence mode, with an integrating gate of 10 μs.

* Corresponding author. Tel: +36-72-327622/4399; fax: +36-72-501528; e-mail: erostyak@fizika.jpte.hu

1010-6030/98/$19.00
PII S1010-6030(98)00235-4

Table 1
Formulas of mixed complexes of Eu/CA and Gd/CA

Serial number	Chemical formula
1	$(C_6H_5CH{=}CHCOO)_3(Eu_{1.0}Gd_{0.0})$
2	$(C_6H_5CH{=}CHCOO)_3(Eu_{0.9}Gd_{0.1})$
3	$(C_6H_5CH{=}CHCOO)_3(Eu_{0.8}Gd_{0.2})$
4	$(C_6H_5CH{=}CHCOO)_3(Eu_{0.7}Gd_{0.3})$
5	$(C_6H_5CH{=}CHCOO)_3(Eu_{0.6}Gd_{0.4})$
6	$(C_6H_5CH{=}CHCOO)_3(Eu_{0.5}Gd_{0.5})$
7	$(C_6H_5CH{=}CHCOO)_3(Eu_{0.4}Gd_{0.6})$
8	$(C_6H_5CH{=}CHCOO)_3(Eu_{0.3}Gd_{0.7})$
9	$(C_6H_5CH{=}CHCOO)_3(Eu_{0.2}Gd_{0.8})$
10	$(C_6H_5CH{=}CHCOO)_3(Eu_{0.1}Gd_{0.9})$
11	$(C_6H_5CH{=}CHCOO)_3(Eu_{0.0}Gd_{1.0})$

3. Results and discussion

3.1. Excitation and emission spectra

The excitation bands of the ligand and the Eu^{3+} can be well identified on the excitation spectra (Fig. 1).

The ligand bands are centered at 240 nm and 335 nm. A slight slope can be seen over 370 nm, which is typical for powder samples and originates mainly from the non-monomer forms of the complexes. The Gd^{3+} ions do not take part

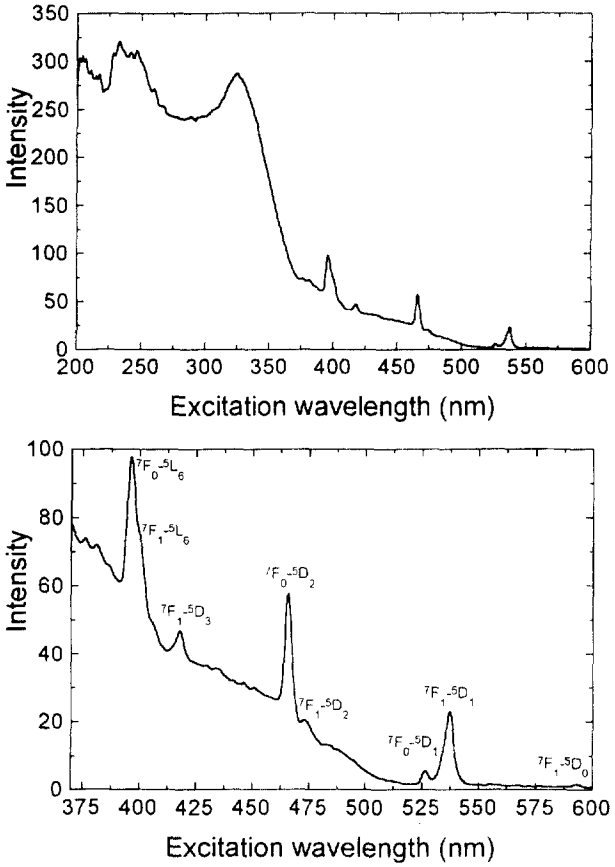

Fig. 1. Typical excitation spectra of Eu/Gd/CA mixed complex. $\lambda_{em} = 616$ nm. 70% Eu^{3+}, 30% Gd^{3+}. Fresh sample.

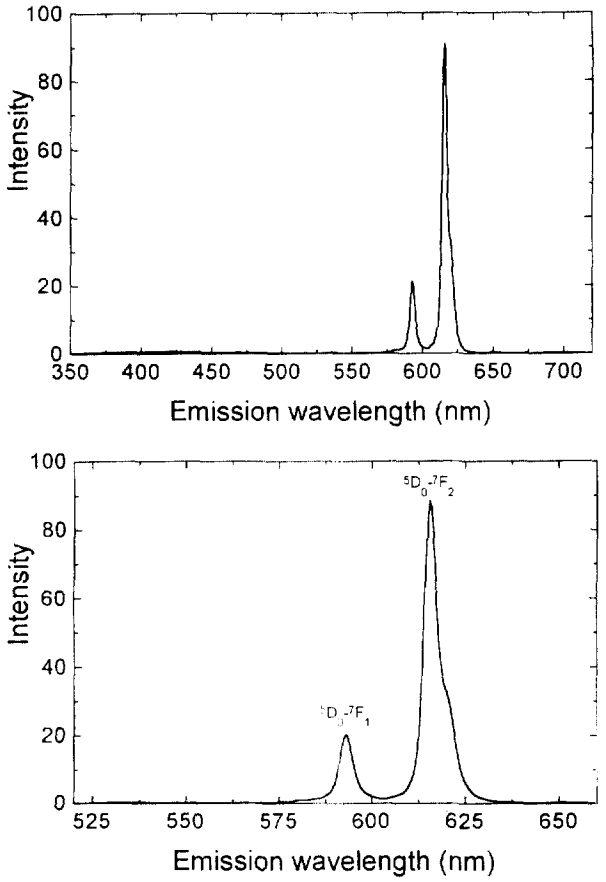

Fig. 2. Typical emission spectra of Eu/Gd/CA mixed complex. $\lambda_{ex} = 240$ nm. 70% Eu^{3+}, 30% Gd^{3+}. Fresh sample.

in the energy transfer processes due to their well-known electronic structures. The Eu^{3+} ions can be excited to their $^5D_0$,$^5D_1$,$^5D_2$,$^5D_3$ and $^5L_6$ levels. The emission was measured at 616 nm, which means that all of the excited states mentioned in the previous sentence relax through the $^5D_0$ level. In some complexes, a ligand-to-metal charge transfer state (CT) can be assumed, which give a very effective relaxation way from the levels above $^5D_2$ [14] especially at room temperature. The presence of ^7F_i–^5D_j ($i = 0, 1$; $j = 1, 2, 3$) and ^7F_i–$^5L_6$ transitions in the excitation spectra means that there is not any ligand-to-metal CT state, where the excited states above $^5D_2$ level could relax via crossover to.

In the emission spectra (Fig. 2), two bands of Eu^{3+} can be seen ($^5D_0$–$^7F_1$ and $^5D_0$–$^7F_2$ transitions). Let us note that the $^5D_0$–$^7F_0$ transition (580 nm), which is always present in solution has an intensity being under the detection limit. Moreover, the ligand has a broad, very weak emission band around 400 nm.

The shape and relative intensity of Eu^{3+} emission bands does not depend on the excitation wavelength. From the higher excited states of Eu^{3+} there are not any luminescence emission, these states relax either to the lowest lying excited state ($^5D_0$) or to the ground state ($^7F_0$) only by non-radiative transitions (In solution the luminescence from a higher

excited state can in some cases be observed [15]). Although the asymmetry in the $^5D_0$–$^7F_1$ transitions might indicate the presence of more than one emitting species, the decay curves can be well fitted with a single term of exponentials (see pre).

3.2. Photochemical degradation

Irradiating the samples by UV light having wavelength of shorter than 330 nm the emission intensity (measured at 616 nm) decreases in time. It means that a photochemical degradation occurs in the irradiated samples. Let us compare the excitation spectra of the fresh and irradiated samples (Fig. 3A). The wavelength of irradiating light was 240 nm and the time of irradiation was 1800 s (It was a pulsed irradiation by flashes of 10 μs using 50 Hz repetition rate!).

Both the absolute and relative degree of photodegradation is much higher in the case of low Eu^{3+} content then in the case of high Eu^{3+} content. As it can be well seen from the difference of excitation spectra (Fig. 3B) the excitability of sample at the 240 nm excitation band decreases especially in the case of sample of low Eu^{3+} content. Fig. 4A and B show how the photodegradation develops in time.

The curves of Fig. 4A and B are non-exponentials and has a characteristic time of about 4 min. Displaying the emission intensities before and after irradiation (Fig. 5A and B) it can

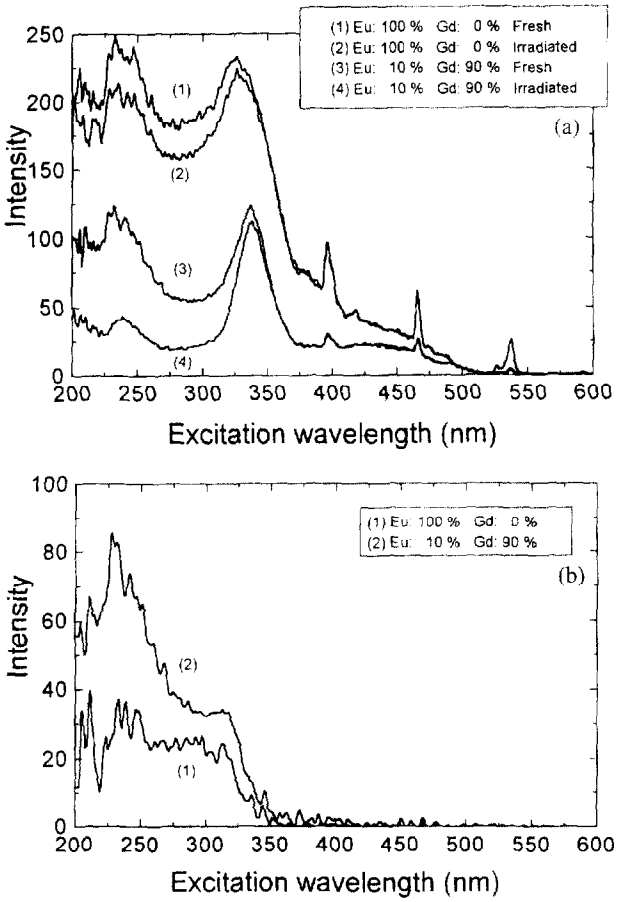

Fig. 3. (a) Excitation spectra of fresh and irradiated samples. (b) Differences of excitation spectra. Fresh–irradiated.

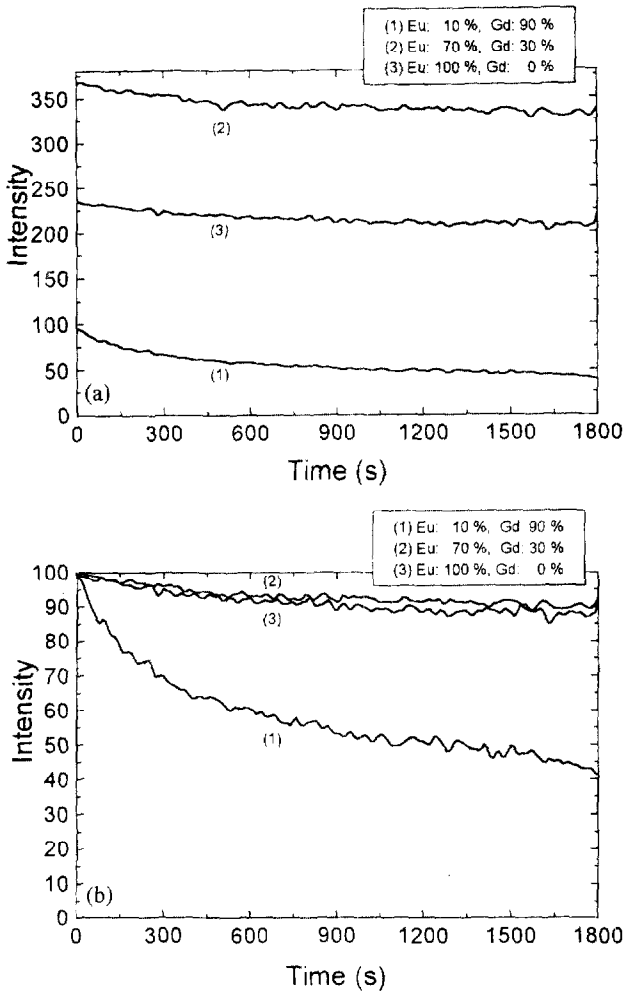

Fig. 4. Decrease of emission intensity under irradiation. (a) Absolute intensities. (b) Relative intensities. λ_{ex} = 240 nm, λ_{em} = 616 nm.

be clearly seen that the samples of low Eu^{3+} content loose even more than 50% of its emission intensities. At high Eu^{3+} content this decrease is not more than 10%. On this type of figures, the independent variable is C_{Eu}, which stands for the number of Eu^{3+} ions among every hundreds of lanthanide ions.

Comparing the curves of Fig. 6A (λ_{ex} = 337 nm) and Fig. 6B (λ_{ex} = 240 nm), it can be seen clearly that the photodegradation is significant only in the case of shorter excitation wavelength. (The curves (1) and (2) of Fig. 5A are displayed also on Fig. 6B for a later discussion of other point of view.)

The main reason of this photodegradation effect is probably that the double-bonds of the CA ligands are cut by the short wavelength UV light having high enough energy. On the other hand, the reason, why the degree of photodegradation is higher at low Eu^{3+} concentration, is not clear yet, because Gd^{3+} has generally a very similar coordination behavior as Eu^{3+}. The effect found needs further studies.

3.3. Sensitized luminescence of Eu^{3+}

The decay of Eu^{3+} luminescence can be fitted as one-exponential:

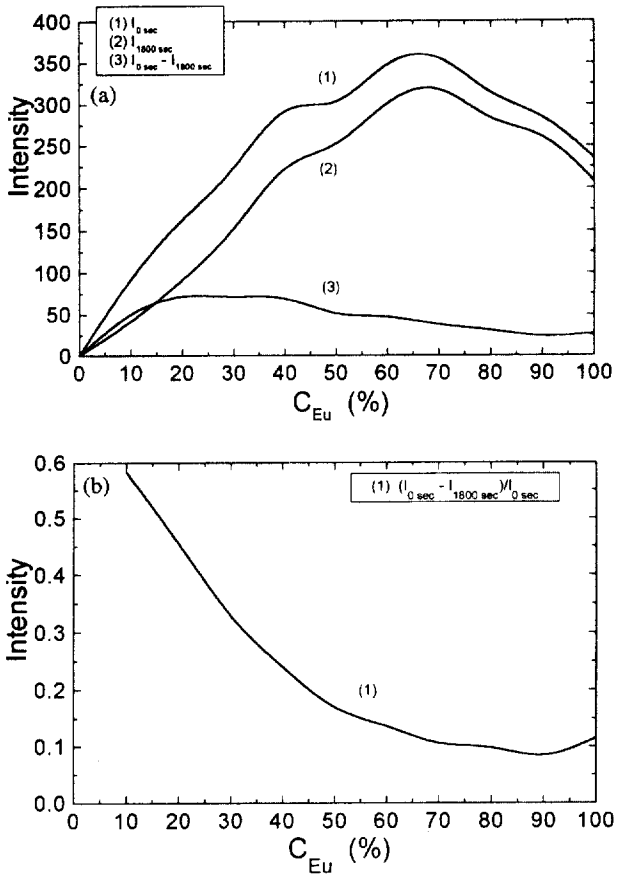

Fig. 5. (a) Emission intensities before and after irradiation. (b) Relative change of emission intensities. $\lambda_{ex} = 240$ nm, $\lambda_{em} = 616$ nm.

$$I(t) = I_0 e^{-t/\tau}, \quad (1)$$

where I_0 stands for the intensity right after the excitation (initial intensity) and τ stands for the decay time. Integrating Eq. (1), one can get the integrated emission intensity, the data points of measured spectra. The integrated emission intensity is equal to the product of the initial intensity and the decay time:

$$\int_0^\infty I(t)\mathrm{d}t = I_0\tau. \quad (2)$$

The integrated emission intensity shows a very interesting dependence on the Eu^{3+} contents of the samples (Fig. 6A and B).

Increasing the Eu^{3+} content the emission intensity increases monotonically, but not linearly up to the ratio of 70% Eu^{3+}/30% Gd^{3+}. The further increase of Eu^{3+} content results in a slight decrease in the integrated emission intensity. In the case of excitation wavelength of 337 nm, the fresh and irradiated samples show very similar values (Fig. 6A). The difference between them is only a few percent. In the case of excitation wavelength of 240 nm the difference in the integrated emission intensities between fresh and irradiated samples is higher (Fig. 6B). But all of the curves of Fig. 6A and B show similar intensity dependence on the Eu^{3+} content of the samples. Now let us analyze the dependence of initial intensities and decay times on the Eu^{3+} content (Fig. 7), which one of them is responsible for the shape of curves of Fig. 6A and B.

From Fig. 7A, it can be well seen that the dependence of initial intensities is very similar to the dependence of integrated emission intensities on the Eu^{3+} content (Fig. 6A). The decay time depends much less on the Eu^{3+} content (the maximum and minimum values of it differ by not more than 20%), but anyway this dependence is also significant. Thus it can be concluded that although the initial intensities are primarily responsible for the shape of the curves of integrated emission intensities, the decay time gives also a non-negligible contribution. Both of them reach their maximum values at 70% Eu^{3+} content. The initial intensities are proportional to the yield of energy transfer towards Eu^{3+}. The decay times are related to the quenching and shielding processes influencing the emitting excited state of Eu^{3+}. That is, both the most efficient energy transfer and the lowest rate of quenching of $^5D_0$ level occur at about 70% Eu^{3+} content.

Now let us focus on the quantitative details of intramolecular energy transfer (IntraMET) and intermolecular energy transfer (InterMET). Because the lifetime of Eu^{3+} is longer than the lifetime of CA by many orders of magnitude, thus the result of energy transfers can be seen purely on the curve of initial intensities. In the case of a fresh sample it is curve

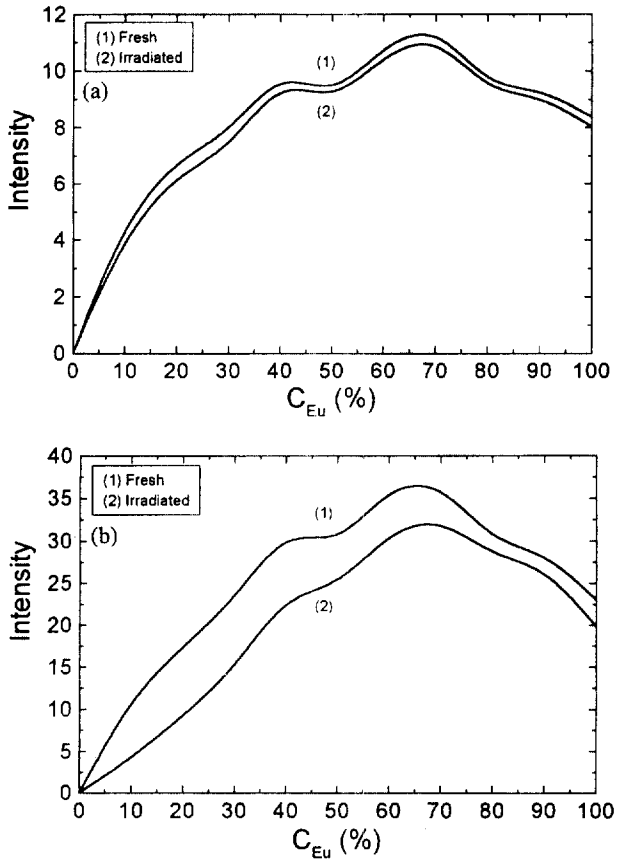

Fig. 6. $\Sigma I = I_0\tau$ Integrated emission intensities. (a) $\lambda_{ex} = 337$ nm. (b) $\lambda_{ex} = 240$ nm. $\lambda_{em} = 616$ nm in both cases.

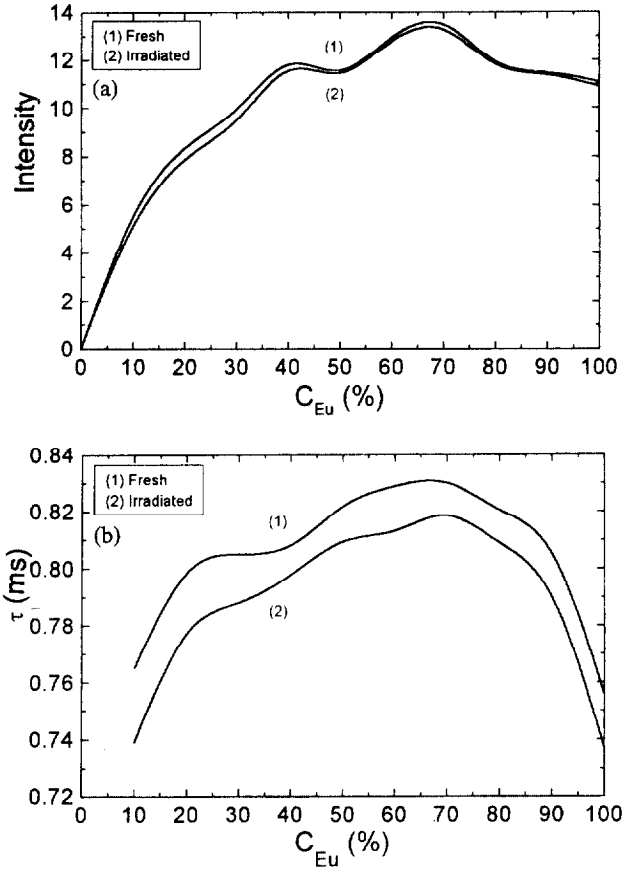

Fig. 7. (a) I_0 Initial intensities. (b) τ Decay times. $\lambda_{ex}=337$ nm. $\lambda_{em}=616$ nm.

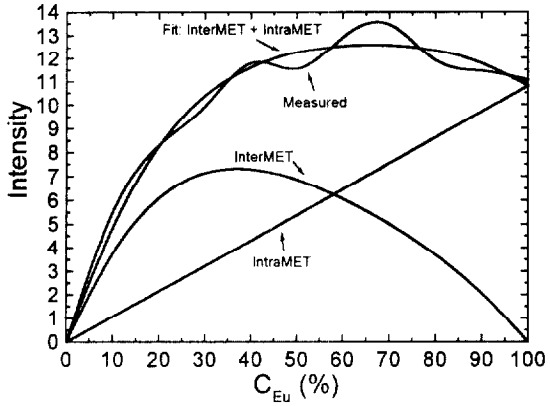

Fig. 8. Fit for measured initial intensities. $\lambda_{ex}=337$ nm. $\lambda_{em}=616$ nm.

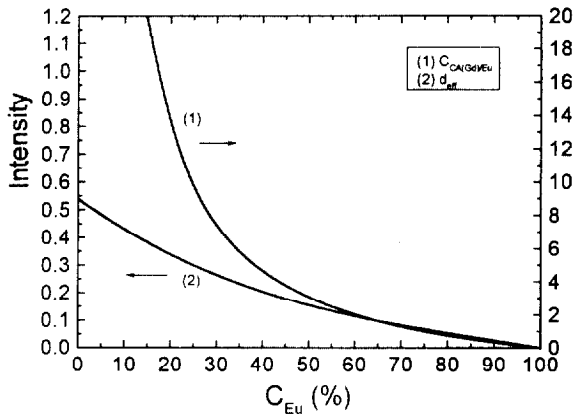

Fig. 9. (1) Number of Gd-bonded CAs per Eu^{3+} ions. (2) Factor proportional to the average distance of InterMET.

(1) of Fig. 7A. On Fig. 8, it is also shown and is named Measured. For calculation it is fitted by polynomials (curve: Fit). This initial intensity of luminescence of Eu^{3+} derives from IntraMET and InterMET:

$$I_{Eu}=I_{IntraMET}+I_{InterMET}. \quad (3)$$

In the case of IntraMET, the energy is transferred from the CAs bonded to a Eu^{3+} (let $C_{CA(Eu)}$ stand for their number) towards that Eu^{3+}. In the case of InterMET the energy is transferred from the CAs bonded to a Gd^{3+} (let $C_{CA(Gd)}$ stand for their number) towards a Eu^{3+}. For later calculations, let us calculate $C_{CA(Gd)/Eu}$, the number of Gd^{3+}-bonded CAs per Eu^{3+}:

$$C_{CA(Gd)/Eu}=\frac{C_{CA(Gd)}}{C_{Eu}}=\frac{C_{CA}}{C_{Eu}}-3, \quad (4)$$

where $C_{CA}=C_{CA(Eu)}+C_{CA(Gd)}=300$ is the number of the CAs for every hundreds of lanthanide ions.

The luminescence intensity deriving from IntraMET (on Fig. 8 it is shown as a straight line) is supposed to be proportional to the number (or—if you like—concentration) of Eu^{3+} ions:

$$I_{IntraMET}=K_1 C_{Eu}, \quad (5)$$

where K_1 is a constant. The difference between the total initial luminescence intensity and the intensity deriving from IntraMET is the intensity deriving from InterMET. It is also shown on Fig. 8. Because the Eu^{3+} ions are the final emitters, let us write it as a product of C_{Eu} and an other factor d_{av}:

$$I_{InterMET}=C_{Eu}d_{av}. \quad (6)$$

The curve of d_{av} is shown on Fig. 9. d_{av} is the highest when the concentration of Eu^{3+} tends to zero. Increasing C_{Eu}, the value of d_{av} decreases monotonically. It is because the Eu^{3+} ions compete each other, and at higher concentration of Eu^{3+} the InterMET is effective only the from Gd-bonded CAs being in the closest proximity of the Eu^{3+} complex. Thus d_{av} is proportional to the average distance of InterMET. Because the exact types and roles of possible InterMET processes is not known at this moment, it can not be concluded any quantitative meaning to the polynomial fit describing the shape of d_{av}:

$$d_{av}=0.42035-0.00997C_{Eu}+1\times10^{-4}C_{Eu}^2-4.3303\times10^{-7}C_{Eu}^3. \quad (7)$$

Now let us compare the shape of curves of d_{av} and $C_{CA(Gd)/Eu}$ (Fig. 9). It can be seen well that in the case of $C_{Eu}>50\%$ the two curves goes quite together. At lower concentration of Eu^{3+} $C_{CA(Gd)/Eu}$ (which is the number of Gd-bonded CAs

per Eu^{3+} ions) tends to the infinity but d_{av} tends to a finite number. That is the CAs being farther and farther from a Eu^{3+} ion can transfer their energy towards a Eu^{3+} ion by drastically less and less efficiency.

The most possible types of InterMET can be dipole–dipole, dipole–quadrupole interactions and energy migration. To distinguish between them quantitatively needs further studies which can base on the data presented here.

4. Conclusions

The Eu/Gd/CA complex is a promising light-converting material. The photoemission of it occurs in 98% at the two main emission lines of Eu^{3+} (592 nm, 616 nm). From all of the ligand states and the higher-lying excited states of Eu^{3+} there is effective energy transfer towards the $^5D_0$ level. The integrated emission intensity of mixed complexes depend on the ratio of Eu^{3+}/Gd^{3+} contents. Both the maximal emission intensity and the lowest rate of quenching of the $^5D_0$ level was found to be at about 70% Eu^{3+} content. It means that the energy transfer is the most efficient when the CA/Eu^{3+} ratio of the solid sample is about 4.3:1 [which is higher than the stoichiometric 3:1 of $Eu^{3+}/(CA)_3$].

The energy transfer consists of IntraMET and InterMET. The IntraMET can be supposed to be proportional to the concentration of Eu^{3+}. The luminescence intensity deriving from InterMET can be written as a product of the concentration of Eu^{3+} and a factor which is proportional to the average distance of InterMET. The lower the C_{Eu}, the higher the d_{av} is. Nevertheless, the efficiency of InterMET from longer distances decreases drastically.

The samples show some photochemical degradation under UV irradiation of short wavelength. It is significant at low Eu^{3+} contents.

The effects found seem to be worth of further studies: (a) at different temperatures; (b) with higher spectral resolution and (c) with better time resolution (on the nanosecond time scale).

Acknowledgements

This work was supported by the National Science and Research Foundation of Hungary under contract No. OTKA-7621.

References

[1] J.C.G. Bünzli, in: J.C.G. Bünzli, G.R. Choppin (Eds.), Lanthanide Probes in Life, Chemical and Earth Sciences, Theory and Practice, Elsevier, Amsterdam, 1989, p. 219.
[2] M. Elbanowski, B. Makowska, J. Photochem. Photobiol. A: Chem. 99 (1996) 85.
[3] I. Hemmilä, J. Alloys Comp. 225 (1995) 480.
[4] E. Soini, Trends Anal. Chem. 9 (1990) 90.
[5] Y.Y. Xu, I. Hemmilä, V.M. Mukkala, S. Holttinen, T. Lövgren, Analyst 116 (1991) 1155.
[6] Y.Y. Xu, I. Hemmilä, Anal. Chim. Acta 256 (1992) 9.
[7] C. de M. Donegá, S.A. Junior, G.F. de Sá, Chem. Commun., 1996, 1199.
[8] J.C.G. Bünzli, E. Moret, V. Foiret, K.J. Schenk, W. Mingzhao, J. Linpei, J. Alloys Comp. 207–208 (1994) 107.
[9] P.A. Tanner, Y.L. Liu, M. Chua, M.F. Reid, J. Alloys Comp. 207–208 (1994) 83.
[10] J. Erostyák, A. Buzády, A. Kaszás, L. Kozma, I. Hornyák, J. Lumin. 72–74 (1997) 570.
[11] J. Li, G. Shen, J. Hu, Y. Zeng, Fresenius J. Anal. Chem. 342 (1992) 552.
[12] G. Zhu, Z. Si, X. Wang, W. Zhu, Anal. Chim. Acta 231 (1990) 295.
[13] J. Georges, Analyst 118 (1993) 1481.
[14] M.T. Berry, P.S. May, H. Xu, J. Phys. Chem. 100 (1996) 9216.
[15] J. Erostyák, A. Buzády, L. Kozma, I. Hornyák, Spec. Lett. 28 (3) (1995) 473.